CODEN IEJMAT *Internet Electronic Journal of Molecular Design* **2008**, *7*, 38–46 ISSN 1538–6414
BioChem Press http://www.biochempress.com

Inter*net* Electronic Journal of Molecular Design

February 2008, Volume 7, Number 2, Pages 38–46

Editor: Ovidiu Ivanciuc

3D–QSAR (Quantitative Structure–Activity Relationships) Studies on Urea Derivatives as Inhibitors of p38 MAP Kinase

Rituparna Sarma,[1] Sharat Sinha,[1] Muttineni Ravikumar,[1] Madala Kishore Kumar,[1] and Shaik Mahmood [2]

[1] Biocampus, S–1, Phase–1, Technocrats Industrial Estate, Balanagar, Hyderabad 500 037, A.P., India

[2] Bioinformatics Division, Environmental Microbiology Lab, Department of Botany, Osmania University, Hyderabad 500 007, A.P., India

Received: October 90, 2007; Revised: January 24, 2008; Accepted: February 16, 2007; Published: February 29, 2008

Citation of the article:
R. Sarma, S. Sinha, M. Ravikumar, M. K. Kumar, and S. Mahmood, 3D–QSAR (Quantitative Structure–Activity Relationships) Studies on Urea Derivatives as Inhibitors of p38 MAP Kinase, *Internet Electron. J. Mol. Des.* **2008**, *7*, 38–46, http://www.biochempress.com.

Inter*net* Electronic Journal of Molecular Design

BioChem Press
http://www.biochempress.com

3D–QSAR (Quantitative Structure–Activity Relationships) Studies on Urea Derivatives as Inhibitors of p38 MAP Kinase

Rituparna Sarma,[1,*] Sharat Sinha,[1] Muttineni Ravikumar,[1] Madala Kishore Kumar,[1] and Shaik Mahmood [2]

[1] Biocampus, S–1, Phase–1, Technocrats Industrial Estate, Balanagar, Hyderabad 500 037, A.P., India

[2] Bioinformatics Division, Environmental Microbiology Lab, Department of Botany, Osmania University, Hyderabad 500 007, A.P., India

Received: October 90, 2007; Revised: January 24, 2008; Accepted: February 16, 2007; Published: February 29, 2008

Internet Electron. J. Mol. Des. **2008**, *7* (2), 38–46

Abstract

Motivation. Inhibition of the p38 MAP kinase pathway has been shown to be beneficial in the treatment of inflammatory diseases. A three–dimensional quantitative structure–activity relationship (3D–QSAR) model, based on molecular field analysis (MFA), was developed for 41 urea derivatives that are inhibitors of p38 mitogen–activated protein kinase (p38 MAPK). The 3D–QSAR model was developed using 32 compounds and its predictive ability was assessed using a test set of 9 compounds.

Method. MFA studies were performed using the QSAR module of Cerius^2.

Results. The predictive 3D–QSAR model has a conventional $r^2 = 0.901$ and a cross–validated coefficient $r^2_{cv} = 0.799$. The model was able to efficiently predict the activities of the compounds of the test set ($r^2_{pred} = 0.740$), suggesting that it can be used for the development of new p38 MAPK inhibitor candidates, useful for treatment of chronic inflammatory states.

Conclusions. The structural features indicated by this 3D–QSAR analysis provide a helpful guideline to design novel compounds with inhibitory activities against p38 MAPK.

Keywords. p38 MAP kinase, QSAR, MFA, urea derivatives.

Abbreviations and notations

MFA, Molecular Field Analysis	QSAR, quantitative structure–activity relationships
TNF, Tumor necrosis factor	IL, Interleukin
SAR, Structure–Activity Relationship	MCS, minimum common subgraph
r^2_{cv}, cross–validated r^2	R^2, conventional r^2
PRESS, predicted sum of squared residuals	R^2_{bs}, bootstrap r^2
r^2_{pred}, predictive r^2	

* Correspondence author; E–mail: rituparna.sarma@gmail.com.

1 INTRODUCTION

p38 MAP kinase is a member of Ser/Thr kinase family [1] of the mitogen–activated protein (MAP) kinase super family [2,3,4,5]. p38 MAP kinase plays a very important part in diseases, such as asthma, osteoarthritis and rheumatoid arthritis, chronic inflammatory autoimmune diseases. Therefore, the inhibition of p38 MAP kinase would potentially prevent the underlying pathophysiology in the inflammatory diseases, which makes p38 MAP kinase an attractive target for drug discovery [6,7]. The pyridinylimidazole compounds, exemplified by SB203580 (Figure 1), were originally developed as inflammatory cytokine synthesis inhibitors, and were later identified as selective inhibitors of p38 MAP kinase. Thereafter, structurally diverse p38 MAP kinase inhibitors have been synthesized and tested extensively to seek potential therapy for inflammatory diseases resulting from excess cytokine production.

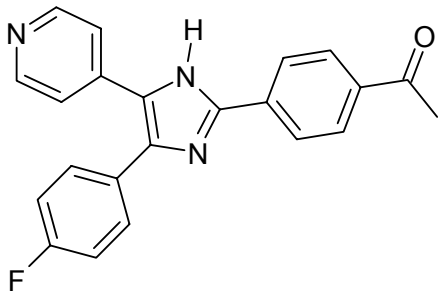

Figure 1. SB203580, an inhibitor of p38 MAP kinase.

A QSAR study for the above mentioned series of compounds was used to rationalize structural requirements for increasing binding affinity of the compounds to p38 MAP kinase. A QSAR study sought to explain and predict activities of series of congeners by utilizing empirical descriptors. QSAR modeling results in a quantitative correlation between chemical structure and biological activity [8]. Conventional QSAR relies on descriptors to characterize structures [9,10]. The factors contributing to the biological activity can be understood through use of different physicochemical descriptors in the generation of QSAR models [11,12]. Further, QSAR enables to establish *in silico* quantitative models to predict the activity of novel molecules prior to their synthesis and simultaneously provide deeper insight into the mechanism of drug–receptor interaction [13,14].

In the present study, we have gone beyond the mentioned studies to develop 3D–QSAR models, MFA [15,16,17] on a series of urea derivatives in order to provide key structural features required to design p38 MAP kinase inhibitors to efficiently predict the biological activity of compounds not included in the training set.

Table 1. Structures and Activities of all Chemical Compounds

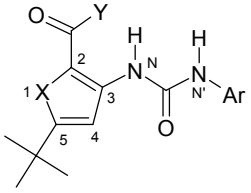

Main scaffold

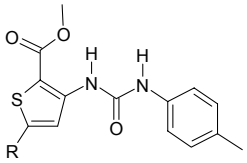

A

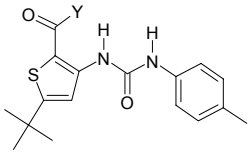

B

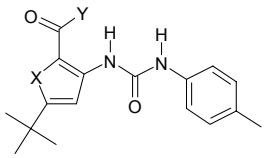

C

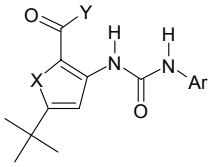

D

Comp.	Scaffold	R	Y	X	Ar	Experimental	
						IC_{50} (nM)	pIC_{50}
1	A	$C(CH_3)_3$	–	–	–	413	6.38
2	B	–	OEt	–	–	3020	5.51
3	B	–	OPr	–	–	482	6.31
4	B	–	$O(CH_2)_2OH$	–	–	57	7.24
5	B	–	$O(CH_2)_3OH$	–	–	56	7.45
6	B	–	$O(CH_2)_2OCH_3$	–	–	464	6.33
7	B	–	$OCH_2CO_2CH_3$	–	–	5310	5.27
8	C	–	NHMe	S	–	34	7.46
9	C	–	OMe	O	–	73	7.13
10	C	–	NHMe	O	–	32	7.40
11	C	–	OMe	NH	–	33	7.48
12	D	–	OMe	S	4–C_2H_5–Ph[a]	660	6.18
13	D	–	NHMe	S	4–C_2H_5–Ph	119	6.92
14	D	–	NHMe	S	4–$_i$Pr[b]	270	6.56
15	D	–	OMe	S	4–F–Ph	830	6.08
16	D	–	NHMe	S	4–F–Ph	88	7.05
17	D	–	OMe	S	4–NH_2–Ph	750	6.12
18	D	–	OMe	S	4–OH–Ph	610	6.21
19	D	–	OMe	S	2,3–Cl–Ph	180	6.73
20	D	–	OMe	O	4–F–Ph	210	6.67
21	D	–	OMe	NH	4–F–Ph	42	7.37
22	D	–	OMe	NH	2–Cl–Ph	60	7.22
23	D	–	OMe	NH	3–Cl–Ph	27	7.56
24	D	–	OMe	NH	4–Cl–Ph	43	7.35
25	D	–	OMe	NH	2,3–Cl–Ph	6	8.22
26	D	–	NHMe	NH	2,3–Cl–Ph	44	7.35
27	D	–	OMe	NH	1–naphthyl	12	7.92
28	D	–	NHMe	NH	1–naphthyl	28	7.55
29	D	–	OMe	NMe	Ph	947	6.02
30	D	–	OMe	NMe	4–F–Ph	663	6.17
31	D	–	OMe	NMe	2,3–Cl–Ph	387	6.41
32	D	–	OMe	NMe	1–naphthyl	253	6.58
33	D	–	OMe	O	3,4–Cl–Ph	1200	5.92
34	B	–	O_iPr	–	–	741	6.13
35	A	NH_2	–	–	–	441	6.35
36	D	–	OMe	NMe	4–CH_3–Ph	400	6.30
37	D	–	OMe	S	Ph	290	6.53
38	D	–	OMe	S	4–Cl–Ph	220	6.65
39	C	–	NHMe	NH	–	67	7.17
40	D	–	OMe	NH	Ph	44	7.35
41	D	–	OMe	O	2,3–Cl–Ph	32	7.48

[a] Ph = Phenyl
[b] $_i$Pr = Isopropyl

2 MATERIALS AND METHODS

2.1 Experimental Section

A data set of 41 compounds reported as p38α MAP kinase inhibitors was collected from the literature [18]. The inhibitory activities were expressed as IC_{50} [19] (concentration of the compound required to inhibit *E. coli* p38α MAP kinase activity by 50%). These IC_{50} values were further converted into the corresponding pIC_{50} (–log IC_{50}) values (Table 1). All the compounds were built using the co–ordinates of the ligand present in crystal structure of p38 MAP kinase (PDB ID 1W82 [20]. The molecules were later minimized using steepest descent algorithm using a gradient convergence value of 0.001 kcal/mol. Partial atomic charges were calculated using the Gasteiger method [21]. Furthermore, optimization of the compound geometry was done using the MOPAC 6 package using the semi–empirical AM1 Hamiltonian [22].

2.2 Alignment

All the molecules were aligned using the shape reference alignment option [23] in the QSAR module within Cerius^2 [24]. The most active compound **25** was used as shape reference compound for superposing the rest of the molecules. The aligned molecules are shown in Figure 3. MFA studies were performed using QSAR module of Cerius^2. The negative logarithm of the biological activities of all 32 molecules in the training set and 9 molecules in the test set were chosen as the dependent variables (Tables 3 and 4). By using G/PLS regression method, multiple QSAR equations were generated with over 50,000 generations from which one equation with the highest r^2, r^2_{cv} and lowest PRESS value was considered for further discussion. Cross–validation was done with the leave–one–out procedure. PLS analysis was scaled, with all variables normalized to a variance of 1.0.

3 RESULTS AND DISCUSSION

The training set consisted of 32 compounds while the model was validated using an external set of 9 compounds. The statistical details of the 3D–QSAR model are shown in Eq. (1). Tables 3 and 4 show the actual and predicted activities obtained from MFA 3D–QSAR models for the training and the test set molecules. Figure 2 shows the graph of actual versus predicted pIC_{50} values of the training set and the test set molecules for 3D–QSAR models. The cross–validated r^2_{cv} for MFA model was 0.799, while the non–cross–validated r^2 with five components was 0.901. The boot strapping r^2_{bs} value was 0.898. The actual and predicted pIC_{50} values of the training set are shown in Table 2. The CH_3 probe represents steric and the H^+ probe represents electrostatic descriptors in the MFA QSAR Eq. (1).

Activity = 3.6421 + 0.074492 * "CH_3/465" + 0.033107 * "H^+/397" – 0.034672 * "CH_3/342" + 0.016262 * "H^+/369" + 0.102862 * "CH_3/359" + 0.016145 * "H^+/422" + 0.063181 * "CH_3/89" – 0.00722 * "H^+/289" (1)

PRESS = 2.664 r^2_{cv} = 0.799 r^2 = 0.901 r^2_{bs} = 0.898 r^2_{pred} = 0.740

where: PRESS, predicted sum of squared residuals; r^2_{cv}, cross–validated correlation coefficient; r^2, conventional correlation coefficient; r^2_{bs}, bootstrap correlation coefficient; r^2_{pred}, predictive correlation coefficient.

The presence of steric descriptor (CH_3/89) with positive coefficient at C^5 position of five member heterocyclic groups explains that, a steric group at this position increases the activity. This is evident in the compounds **1** and **35**. Compound **1** contains a tertiary butyl group at C^5 where as in the compound **35** it is replaced with NH_2, which is responsible for decrease in activity. At the C^2 position of the heterocyclic ring, the presence of steric (CH_3/342) descriptor with negative coefficient and electrostatic (H^+/397) descriptor with positive coefficient indicates that electron withdrawing substituent with less steric environment is favored. It shows that any substituent with O or N will have high activity may be due to hydrogen bond interaction between the substituent and active site amino acids of protein. In compounds **4–6**, when $–O(CH_2)_2OH$ group is replaced with $–O(CH_2)_2OCH_3$, activity substantially decreases. At the N^1 position of the urea group, the appearance of two steric groups (CH_3/465 and CH_3/359) with positive coefficient indicates that bigger steric groups are favorable at this position. Compounds **27** and **28** and which contains naphthalene group at this position shows higher activity when compared to the compound **29**, which has phenyl group. The presence of two electrostatic (H^+/369) descriptors with positive coefficient explains the need of both bulky and electron withdrawing substituent. Substitution of the only phenyl group at this position is having less activity as with the compound **29**. But any electron with drawing group is substituted in phenyl ring shows higher activity (compounds **12–26**). Compound **25** with two Cl on the phenyl ring has highest activity.

Compound **36** was found to be an outlier in the test set of MFA model. Its activity is over predicted. This might be due to the presence of $–CH_2Ph$ group on the N^1 position of the urea group. As described above bulkier groups are favored at this position it shows higher activity, but the actual activity of this molecule is less may be due to the steric clash between methyl of $N–CH_3$ and tertiary butyl group present at 1^{st} and 5^{th} position of pyridine ring respectively.

A high r^2_{cv} alone, however, is not a sufficient criterion for a QSAR model to be robust and highly predictive. The predictive power of the model was therefore validated with the test set molecules. The predictive power of the model generated was calculated with the formula r^2_{pred} = (SD – PRESS)/SD, where SD is the sum of the squared deviations between the biological activities of each molecule and the mean activity of the training set of molecules and PRESS is the sum of squared deviations between the predicted and actual activity values for every molecule in the test set. The prediction of the model was reasonably good with a predictive r^2 (r^2_{pred}) value of 0.740. The predictive r^2 (r^2_{pred} = 0.983) of MFA model was found to be high except for compound **36**.

Table 2. Actual and predicted activities of the training set molecules

Comp.	$pIC_{50\ exp}$	$pIC_{50\ MFA\ pre}$
1	6.38	6.645
2	5.51	5.834
3	6.31	6.262
4	7.24	7.279
5	7.45	6.646
6	6.33	6.328
7	5.27	5.166
8	7.46	7.265
9	7.13	7.108
10	7.40	7.443
11	7.48	7.296
12	6.18	6.555
13	6.92	7.260
14	6.56	6.549
15	6.08	6.257
16	7.05	6.891
17	6.12	6.347
18	6.21	6.492
19	6.73	6.956
20	6.67	6.777
21	7.37	7.329
22	7.22	6.973
23	7.56	6.991
24	7.35	7.116
25	8.22	7.894
26	7.35	7.621
27	7.92	8.377
28	7.55	7.186
29	6.02	7.130
30	6.17	7.197
31	6.41	6.369
32	6.58	8.178

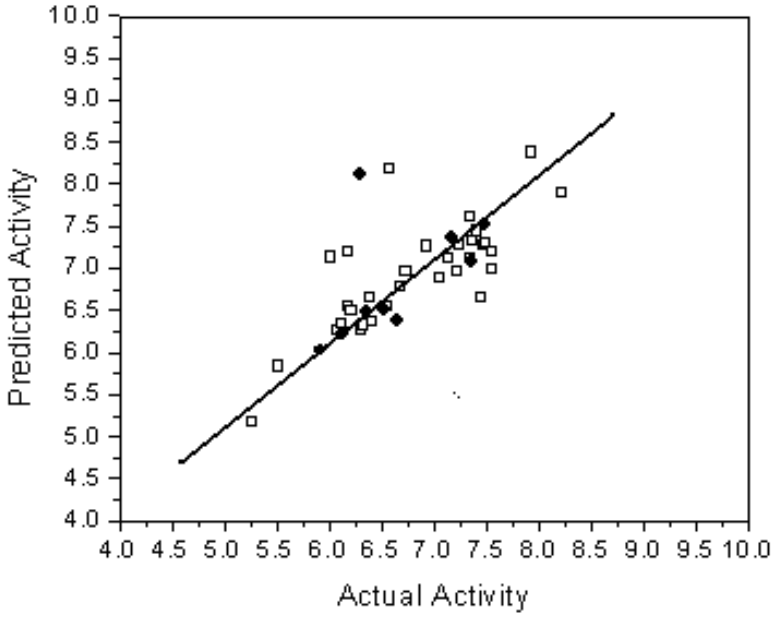

Figure 2. Scatter plots of actual versus predicted activities of Training (□) and test (■) molecules.

Table 3. Actual and predicted activities of the test set molecules

Comp.	$pIC_{50\ exp}$	$pIC_{50\ MFA\ pre}$
33	5.92	6.029
34	6.13	6.219
35	6.35	6.481
36	6.30	8.115
37	6.53	6.512
38	6.65	6.377
39	7.17	7.363
40	7.35	7.083
41	7.48	7.520

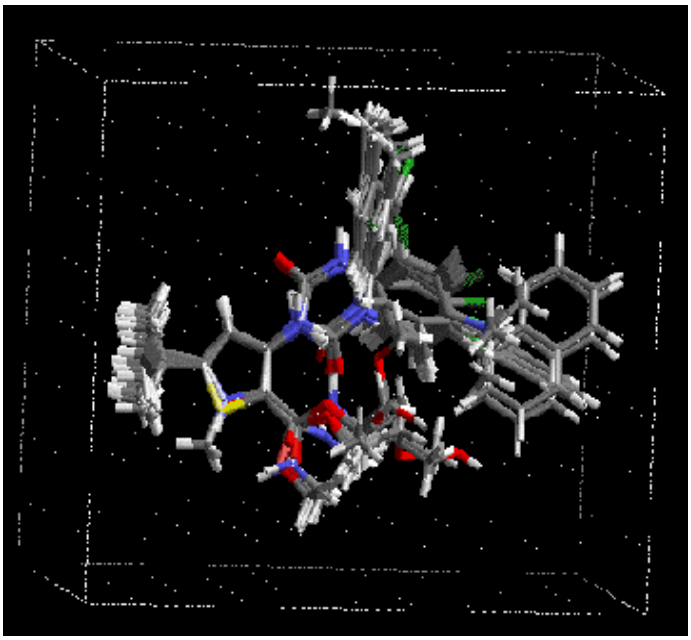

Figure 3. Alignment of study molecules in grid.

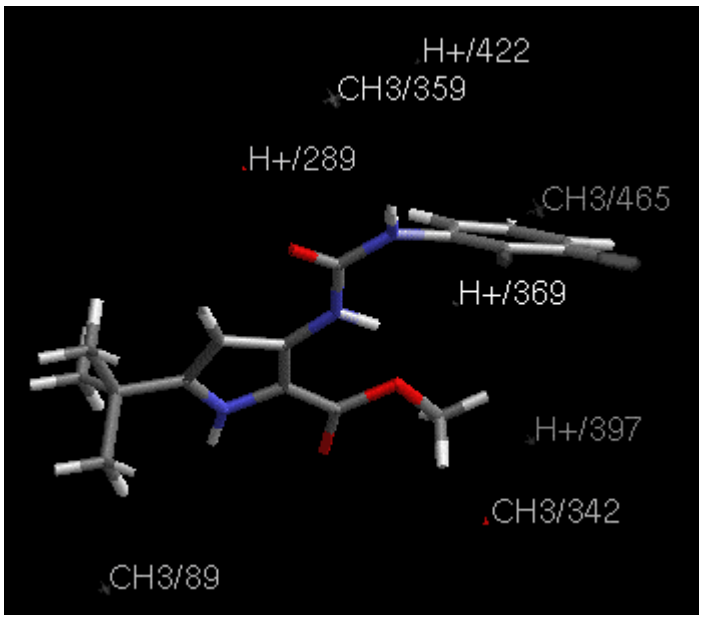

Figure 4. Mapping of 3D–descriptor points in the QSAR equations with most active molecule.

4 CONCLUSIONS

Congeneric data set of 32 compounds as selective p38 MAPK inhibitors was used to generate and validate 3D–QSAR model using MFA methodology. The best predictive model was generated with r^2_{pred} of 0.740 and had the best predictive capacity with a high LOO cross–validated correlation coefficient (r^2_{cv} = 0.799). It was able to predict the inhibitory activities of 9 inhibitors of the p38 MAPK not included in the model construction and offers important structural insight for rational designing novel selective p38 MAPK inhibitors prior to their synthesis. We conclude that the structural features indicated by this 3D–QSAR analysis may provide a helpful guideline to design novel compounds with inhibitory activities against p38 MAPK.

Acknowledgment

The authors thank Dr. J.A.R.P. Sarma, Senior Vice President, GVK Biosciences Pvt. Ltd. for his cooperation and providing software facilities.

5 REFERENCES

[1] P. Sandra, J. P. Maria, M. C. Pedro, S. M. Victoria, R. G. Ana, C. Piero, M. Federico Jr., and M. Cristina, Phosphorylation of p38 by GRK2 at the docking groove unveils a novel mechanism for inactivating p38MAPK, *Curr. Bio.* **2006**, *16*, 2042–2047.

[2] J. C. Lee, J. T. Laydon, P. C. McDonnell, T. F. Gallagher, S. Kumar, D. Green, D. McNulty, M. J. Blumenthal, J. R. Heys, S. W. Landvatter, J. E. Stricker, M. M. McLaughlin, J. R. Siemens, S. M. Fisher, G. P. Livi, J. R. White, J. L. Adams, and P. R. Young, A protein kinase involved in the regulation of inflammatory cytokine biosynthesis, *Nature* **1994**, *372*, 739–746.

[3] J. Hans, J. D. Lee, L. Bibbs, and R. J. Ulevitch, A MAP kinase targeted by endotoxin and hyperosmolarity in mammalian cells, *Science* **1994**, *265*, 808–811.

[4] M. R. S. Nayana, Y. N. Sekhar, N. S. Kumari, S. K. Mahmood, and M. Ravikumar, CoMFA and docking studies on triazolopyridine oxazole derivatives as p38 MAP kinase inhibitors, *Eur. J. Med. Chem.* **2008**, *43*, 1261–1269.

[5] M. R. S. Nayana and Y. N. Sekhar, Comparative Molecular Field Analysis (CoMFA) for p38 Inhibitors, *Internet Electron. J. Mol. Des.* **2007**, *6*, 385–395, http://www.biochempress.com.

[6] F. M. Brennan and M. Feldman, Cytokines in autoimmunity, *Curr. Opin. Immunol.* **1996**, *8*, 872–877.

[7] G. Camussi and E. Lupia, The future role of anti–tumour necrosis factor (TNF) products in the treatment of rheumatoid arthritis, *Drugs* **1998**, *55*, 613–620.

[8] C. Hansch, A quantitative approach to biochemical structure–activity relationships, *Acc. Chem. Res.* **1969**, *2*, 232–239.

[9] A. R. Katritzky and E. V. Gordeeva, Traditional topological indices vs. electronic geometrical and combined molecular descriptors in QSAR/QSPR research, *J. Chem. Inf. Comput. Sci.* **1993**, *33*, 835–857.

[10] H. Van de Waterbeemd, Recent progress in QSAR–technology, *Drug Des. Discov.* **1993**, *9*, 277–285.

[11] Y. N. Sekhar, M. R. S. Nayana, S. K. Mahmood, and M. Ravikumar, Comparative Molecular Field Analysis on quinoline derivatives of Metabotropic glutamate receptor subtype 1, *Chem. Biol. Drug Des.* **2007**, *70*, 511–519.

[12] S. M. Vadlamudi and V. M. Kulkarni, 3D–QSAR of Protein Tyrosine Phosphatase 1B Inhibitors by Genetic Function Approximation, *Internet Electron. J. Mol. Des.* **2004**, *3*, 586–609, http://www.biochempress.com.

[13] P. M. Kumar, C. Karthikeyan, N. S. H. N. Moorthy, and P. Trivedi, Quantitative structure–activity relationships of selective antagonists of glucagon receptor using QuaSAR descriptors, *Chem. Pharm. Bull.* (*Tokyo*) **2006**, *54*, 1586–1591.

[14] M. R. S. Nayana, Y. N. Sekhar, N. S. Kumari, and SK. Mahmood, 3D–QSAR CoMFA Study on Human Glutaminyl Cyclase Inhibitors, *Internet Electron. J. Mol. Des.* **2007**, *6*, 320–330, http://www.biochempress.com.

[15] A. J. Hopfinger, J. S. Tokarsi, and P. S. Charifson (Eds.), Practical Applications of Computer–Aided Drug Design, Marcel Dekker, New York, 1997.

[16] D. Rogers and A. J. Hopfinger, *J. Chem. Inf. Comput. Sci.* **1994**, *34*, 854.

[17] Y. N. Sekhar, M. Ravikumar, M. R. S. Nayana, S. C. Mallena, and M. K. Kumar, 3D–QSAR study on triazafluorenone inhibitors of metabotropic glutamate receptor subtype 1, *Eur. J. Med. Chem.* **2008**, *43*, 1025–

1034.
[18] A. M. Redman, J. S. Johnson, R. Dally, S. Swartz, H. Wild, H. Paulsen, Y. Caringal, D. Gunn, J. Renick, M. Osterhout, J. Kingery–Wood, R. A. Smith, W. Lee, J. Dumas, S. M. Wilhelm, T. J. Housley, A. Bhargava, G. E. Ranges, A. Shrikhande, D. Young, M. Bombara, and W. J. Scott, p38 kinase inhibitors for the treatment of arthritis and osteoporosis: thienyl, furyl, and pyrrolyl ureas, *Bioorg*. *Med*. *Chem*. *Lett*. **2001**, *11*, 9–12.
[19] D. Hammaker, S. Sweeney, and G. S. Firestein, Signal transduction networks in rheumatoid arthritis, *Ann*. *Rheum*. *Dis*. **2003**, *62*, 86–89.
[20] http://www.rcsb.org, PDB 1W82.
[21] J. Gasteiger and M. Marsili, A New Model for Calculating Atomic Charges in Molecules, *Tetrahedron Lett*. **1978**, 3181–3184.
[22] M. J. S. Dewar, E. G. Zoebisch, E. F. Healy and J. J. P. Stewart, *J*. *Am*. *Chem*. *Soc*. **1985**, *107*, 3902.
[23] V. Aparna, J. Jeevan, M. Ravi, G. R. Desiraju, and B. Gopalakrishnan, 3D–QSAR studies on antitubercular thymidine monophosphate kinase inhibitors based on different alignment method, *Bioorg*. *Med*. *Chem*. *Lett*. **2006**, *4*, 1014–1020.
[24] Cerius^2 version 4.8, Accelrys, San Diego, USA, http://www.accelrys.com/cerius2.